

Bulk and surface transitions in asymmetric simple exclusion process: Impact on boundary layers

Sutapa Mukherji and Vivek Mishra

Department of Physics, Indian Institute of Technology, Kanpur 208016, India

(Dated: July 14, 2018)

In this paper, we study boundary-induced phase transitions in a particle non-conserving asymmetric simple exclusion process with open boundaries. Using boundary layer analysis, we show that the key signatures of various bulk phase transitions are present in the boundary layers of the density profiles. In addition, we also find possibilities of surface transitions in the low- and high-density phases. The surface transition in the low-density phase provides a more complete description of the non-equilibrium critical point found in this system.

I. INTRODUCTION

Studies on a certain class of non-equilibrium systems, namely driven diffusive systems, have revealed many features that are unexpected in systems in thermal equilibrium [1, 2]. For example, it is well known that although in thermal equilibrium, one dimensional systems with short-range interaction cannot exhibit phase transition or spontaneous symmetry breaking, certain driven diffusive systems do exhibit such phenomena even in one dimension [3]. Asymmetric simple exclusion processes (ASEP), which involve biased hopping of particles in one direction with hard-core exclusion along a one-dimensional lattice, fall in the class of driven diffusive systems and despite its simplicity, such processes are capable of exhibiting variety of phenomena [4, 5, 6]. Violation of detailed balance due to the presence of a finite particle current makes such systems so special. This, for example, is reflected in the boundary induced phase transitions in ASEP on one-dimensional finite lattice [7], where, unlike equilibrium, the effect of boundaries propagates into the bulk by a finite particle current.

In this paper, we consider a particle non-conserving version of ASEP with open boundaries. Particles, that are injected at one boundary with a rate α , hop forward with rate unity (no backward hopping is allowed) with hard-core exclusion till they reach the other end of the lattice where particles are withdrawn at a rate $1-\gamma$ [8, 9]. In addition, there is particle non-conservation at the bulk due to the possibility of attachment (detachment) of the particles to (from) the lattice with rate $\omega_a(\omega_d)$. With the variation of the injection and withdrawal rates at the boundaries, such systems exhibit different phases which are characterized by the shape of the density profiles and the nature of the current densities[8]. A mean-field analysis, exact for the hard-core case, leads to a rich phase diagram (see figure 1 and 2) compared to systems without particle adsorption/desorption kinetics (Langmuir Kinetics). For example, there is a phase where the density profile exhibits a jump from a low to a high value at some point in the bulk. This new phase known as the shock phase(S) appears in addition to the high(H) and low-density(L) phases where the bulk-density, though not constant, remains above and below half respectively. Al-

though the shock phase is present for both $K = 1$ and $K \neq 1$, with $K = \omega_a/\omega_d$, these two cases are distinctly different since in the first case a special particle-hole symmetry allows a maximal current(M) phase with bulk density equal to $1/2$. M phase and the coexistence of M phase with L and/or H phase (LMH, LM and HM phases) for $K = 1$, differences in the shapes of the phase boundaries and in the nature of the phase transitions in the two cases make the problem altogether nontrivial.

In a recent work [10], Mukherji and Bhattacharjee have studied the phase-transition between low-density and shock phases using boundary layer techniques. Although the phase diagram has been studied numerically or through a direct solution of the mean-field equation earlier, the boundary layer analysis in [10] reveals a new feature that the transition to the S phase from the L phase has a precursor of a critical confinement of a boundary layer near the open end. In addition, this approach provides a general framework for characterizing the transitions for different values of K and also for studying different mean-field models with additional inter-particle interactions. The purpose of the present work is to employ the boundary layer theory to the mean field version of the model to understand various phase transitions from a boundary layer point of view. From this analysis, it becomes clear that the divergences of various length scales associated with the boundary layers indicate the emergence of bulk phase transitions. Our analysis also reveals possibilities of surface transitions within the low- and high-density phases for both $K = 1$ and $K \neq 1$. Except for the analysis of the surface transition, the discussion is primarily limited to $K = 1$ since, for $K = 1$, various phases and phase transitions give more scope for studying the effect of bulk phase transitions on the boundary layers.

The paper is organized as follows. The model and its symmetry properties have been discussed in section II. We discuss the boundary layer analysis for this model in section III. This section is divided into three subsections for the discussion of low-density, high-density, and maximal current related phases. Observations from the above analysis related to the behavior of the boundary layers near the phase boundaries are mentioned in section IV. Finally, we conclude with a summary of our results in

section V.

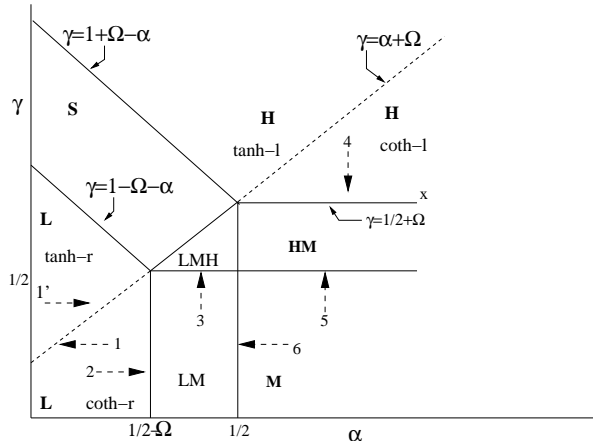


FIG. 1: Phase diagram for $K = \omega_a/\omega_d = 1$ and $\Omega = \omega_d N < .5$. N is the number of lattice points. The coexistence of a maximal-current and a low- or a high-density phase is represented by LM or HM respectively. The coexistence of low-density, maximal-current and high-density phases is similarly represented by LMH. Approach to different phase boundaries are indicated by the paths with arrows. "l" and "r" indicate presence of boundary layers at left and right boundaries respectively. Dashed lines represent surface transition lines.

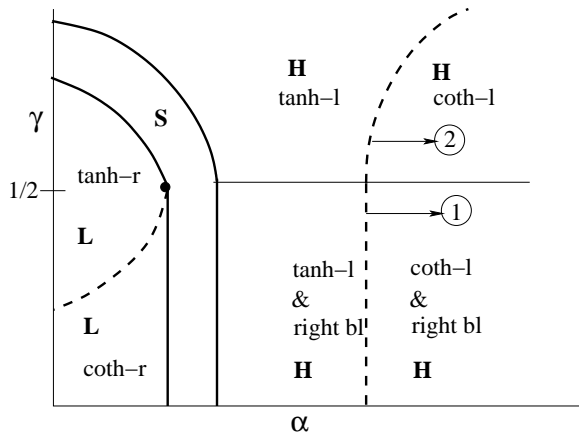


FIG. 2: Phase diagram for $K \neq 1$ and $\Omega = \omega_d N < .5$. N represents the number of lattice points. Dashed lines represent surface transition lines. "bl" implies boundary layer. "l" and "r" indicate presence of boundary layers at left and right boundaries respectively. The filled black circle represents the critical point.

II. MODEL

To describe the ASEP of noninteracting single species of particles, we consider a one dimensional chain of N lattice points and length l . Denoting the occupancy of the i th site by τ_i , which assumes values 0 or 1 depending on whether the site is empty or occupied by a particle,

one may write down the mean-field master equation describing the time evolution of $n_i = \langle \tau_i \rangle$, with $\langle \dots \rangle$ denoting the statistical average, as

$$\frac{dn_i}{dt} = n_{i-1}(1 - n_i) - n_i(1 - n_{i+1}) + \omega_a(1 - n_i) - \omega_d n_i. \quad (1)$$

In this equation, the mean-field approximation is implemented by neglecting correlation as

$$\langle \tau_i \tau_{i+1} \rangle = \langle \tau_i \rangle \langle \tau_{i+1} \rangle. \quad (2)$$

In the large N limit, with the lattice spacing $l/N \rightarrow 0$, one can go over to the continuum by substituting $\langle \tau_{i\pm 1} \rangle = \rho(x, t) \pm \frac{1}{N} \frac{\partial \rho}{\partial x} + \frac{1}{2N^2} \frac{\partial^2 \rho}{\partial x^2} \dots$ where $\rho(x, t)$, is an average density at position $x = i l/N$. The choice $l = 1$ simplifies the notation and restricts the variable x within a range $\{0, 1\}$. Keeping terms up to $O(N^{-2})$, one obtains the following equation describing the shape of the density profile in the steady state

$$\epsilon \frac{d}{dx} f_2(\rho) \frac{d\rho}{dx} + f_1(\rho) \frac{d\rho}{dx} + \Omega f_0(\rho) = 0, \quad (3)$$

with $\Omega = \omega_d N$, $\epsilon = 1/(2N)$ and $f_i(\rho)$ for $i = 0, 1, 2$ given as follows. For the dynamics that we have considered here,

$$f_2(\rho) = 1, \quad f_1(\rho) = 2\rho - 1, \quad f_0(\rho) = K(1 - \rho) - \rho. \quad (4)$$

These f functions, in general, contain information about the dynamics. Such general form for equation (3) will be useful later to make certain general predictions about the boundary layers.

The last term in equation (3) originates from particle adsorption/desorption kinetics and is responsible for the loss of particle number conservation in the bulk. In the absence of this term, the full equation describing the time evolution of $\rho(x, t)$, is expressible as a continuity equation

$$\frac{\partial \rho(x, t)}{\partial t} = - \frac{\partial j}{\partial x}, \quad (5)$$

with the particle current-density j given as

$$j = -\epsilon f_2(\rho) \frac{\partial \rho}{\partial x} - \hat{f}_1(\rho), \quad \text{where} \quad \frac{\partial \hat{f}_i(\rho)}{\partial \rho} = f_i(\rho). \quad (6)$$

In case of equation (4), the current is given by

$$j = -\epsilon \frac{\partial \rho}{\partial x} + \rho(1 - \rho). \quad (7)$$

In the coninum limit ($\epsilon \rightarrow 0$), the current-density $j = \rho(1 - \rho)$ is bounded, $j \leq 1/4$. Since, in the maximal current phase, the bulk density is $\rho = 1/2$, the current-density acquires its maximum value $j = 1/4$ in this phase.

A. symmetries

A better understanding of the phase diagram can be gained from the particle-hole symmetry of the problem. The hopping of a particle in the forward direction is equivalent to the hopping of a hole in the backward direction. Similarly, the injection of particles at one boundary with a certain rate is equivalent to the withdrawal of holes with the same rate. The attachment or detachment of particles can be interpreted as detachment or attachment of holes. The invariance of equation (3) along with f -functions in equation (4) under the transformation

$$\rho \rightarrow 1 - \rho, \quad x \rightarrow 1 - x \quad (8)$$

$$\omega_a \leftrightarrow \omega_d \quad \alpha \leftrightarrow 1 - \gamma. \quad (9)$$

implies that the particle-hole symmetry is respected by the system. This symmetry is not necessarily an obvious property of the system and can be easily destroyed by additional symmetry breaking interaction terms [7, 10].

The situation with $K = 1$ is somewhat special. If the adsorption/desorption kinetics were the only dynamics, the system would have settled in a steady-state density, known as the Langmuir density

$$\rho_l = K/(K + 1) \quad (10)$$

determined from $f_0(\rho) = 0$. If the hopping rules respect conservation, then in the steady state there should be a homogeneous current, if this is the only dynamics. The corresponding density ρ_c is determined from the zero of $f_1(\rho)$, i.e.

$$f_1(\rho_c) = 0. \quad (11)$$

In case of particle-hole symmetry, we expect $\rho_c = 1 - \rho_c$, i.e., $\rho_c = 1/2$ to be special. This as noted earlier is the maximal current state. If $\rho_c = \rho_l$, then $\rho = \rho_c$ becomes a particular solution of the equation. ρ_c is the density at which bulk may allow nonanalytic behavior in the density. This feature is useful for shock formation [10] though the discontinuity is rounded by ϵ dependent term in equation (3). The adsorption/desorption dynamics need not respect this symmetry of hopping and hence the two densities need not be equal. $K = 1$ is a special case where the two densities become equal and the bulk dynamics is symmetric under the transformation $\rho(x) \rightarrow 1 - \rho(1 - x)$.

III. BOUNDARY LAYER ANALYSIS

By changing the boundary values α and γ , one may map out all possible steady state configurations, thereby constituting a “phase diagram” of the non-equilibrium system in the $N \rightarrow \infty$ limit. To understand all these phases, we use a leading order boundary layer analysis that provides a systematic way to generate an uniform approximation of the solution of equation (3). In all the

phases, the density profile over almost the entire space, is described by the solution of the first order equation obtained by ignoring the second derivative term ($\epsilon \rightarrow 0$) in equation (3). This solution, known as the outer solution, is not, in general, expected to satisfy both the boundary conditions. In order to satisfy the boundary conditions appropriately, there appear special regions with boundary layers or shocks. Description of these special regions requires going beyond the first order equation. The solutions describing the boundary layers or shocks are known as inner solutions. The constants in different solutions of the differential equations are determined either by the boundary conditions or by smooth joining of the inner and outer solutions.

The low and high-density phases are related to each other due to particle-hole symmetry and does not require any separate treatment. The difference between the low-density and the maximal current phase arises from the outer solution itself. The outer solutions, solutions of the first order equation (equation (3) in the limit $\epsilon \rightarrow 0$), are

$$\rho_{1,\text{out}} = 1/2, \quad \rho_{2,\text{out}} = \Omega x + c, \quad \text{for } K = 1 \quad (12)$$

$$\text{and } \Omega x = g(\rho_{\text{out}}) - c, \quad \text{with } (13)$$

$$g(\rho) = \frac{1}{1 + K} \left(2\rho + \frac{K - 1}{K + 1} \log[K - (1 + K)\rho] \right) \quad (14)$$

for $K \neq 1$.

Here, c is an unknown constant to be determined from the boundary condition. In the low- and high-density phases, the density profile, over almost the entire space, is described by the linear solution in equation (12) for $K = 1$ or by the solution in equation (14) for $K \neq 1$. The maximal current phase, present only for $K = 1$, has a constant density profile described by the outer solution $\rho_{1,\text{out}}$. In the phase diagram for $K = 1$, there are other regions with coexistence of the maximal current phase with low- or high-density phases or both. The density profile in these phases has constant part $\rho_{1,\text{out}}(x) = 1/2$ as well as linear parts $\rho_{2,\text{out}} = \Omega x + c$ with different parts joined smoothly through specific inner solutions.

The scheme to find the inner solution varies depending upon the kind of matching conditions the inner solution has to satisfy. The procedure to find out the inner solution for L/H phases is different from that for phases involving M phase. The difference arises because in the later case, the inner solutions are required to saturate to $\rho(x) = 1/2$ at either of the two sides and at this value of ρ , $f_1(\rho) = 0$. In the low- or high-density phases, the boundary layer is not required to saturate to $1/2$. Because of these differences, we discuss, L, H and M-related phases in different subsections.

A. Low-density phase: Surface transition

In the low-density phase, $c = \alpha$ for $K = 1$ and $c = g(\alpha)$ for $K \neq 1$ since the outer solution satisfies the left boundary condition. To find the inner solution, one needs

to express equation (3) in terms of $\tilde{x} = (x - x_d)/\epsilon$, where x_d denotes the location of the solution. In the $\epsilon \rightarrow 0$ limit, the inner solution is the solution of

$$\frac{d\rho_{\text{in}}}{d\tilde{x}} = \frac{F(\rho_{\text{in}})}{f_2(\rho_{\text{in}})}, \quad \text{where} \quad (15)$$

$$F(\rho) \equiv \hat{f}_1(\rho_o) - \hat{f}_1(\rho). \quad (16)$$

The matching condition $\rho_{\text{in}}(\tilde{x} \rightarrow -\infty) = \rho_o \equiv \rho_{2,\text{out}}(x = 1)$ for smooth joining of two solutions has already been incorporated. The inner region obeys the particle conservation condition and the continuity equation demands a homogeneous current. Consequently, the current has to be equal to the bulk current entering the region. This is the content of equations (15) and (16) though derived in a different way.

The condition for saturation of the inner solution as $\tilde{x} \rightarrow \infty$ requires

$$F(\rho) = 0 \quad \text{for } \rho = \rho_s > \rho_o. \quad (17)$$

If $\gamma > \rho_{\text{in}}(\tilde{x} \rightarrow \infty)$, the boundary condition cannot be satisfied by ρ_{in} . As a result, the surface layer deconfines from the surface and enters into the bulk with the outer solution again appearing at the right edge to satisfy the right boundary condition. This mechanism leads to the formation of a shock in the density profile at the bulk. The bulk transition to the shock phase, therefore, has a precursor of deconfinement of the surface layer. Since ρ_o is a function of α , one has a phase boundary on the $\alpha - \gamma$ plane $\gamma = \rho_s(\rho_o(\alpha))$ that separates the low-density phase from the shock phase. From equations (4) and (16), we find $\rho_s = 1 - \rho_o$. Assuming simple zeros for $F(\rho)$, we write

$$F(\rho) = -(\rho - \rho_o)(\rho - \rho_s)\phi(\rho), \quad (18)$$

where $\phi(\rho)$ can be determined using equation (3). This form of $F(\rho)$ is convenient as it yields the length scale associated with the crossover of the surface profile to the bulk profile quite generally. The large \tilde{x} behavior of the inner solution can be found from

$$\frac{d\rho_{\text{in}}}{d\tilde{x}} \sim -\frac{(\rho - \rho_s)}{w(\alpha)}, \quad (19)$$

where

$$w(\alpha) = (\rho_s - \rho_o)^{-1} \frac{f_2(\rho_s)}{\phi(\rho_s)}. \quad (20)$$

Equation (19) shows $w(\alpha)$ as the characteristic length scale for the approach to saturation or to the bulk density. $w(\alpha)$ can be made to diverge by changing α and this locates a critical point on the phase boundary between the low-density and the shock phase. At this critical point (α_c, γ_c) , $\rho_s = \rho_o = \gamma_c$.

Given this form of $F(\rho)$, in the low-density phase, the slope of the inner solution at $x = 1$, i.e. at $\rho = \gamma$, is

positive if $\rho_o < \gamma < \rho_s$ and negative if $\gamma < \rho_o$. Thus, with $\gamma_{\text{sc}} = \rho_o$, there is an increasing solution at $x = 1$ for $\gamma > \gamma_{\text{sc}}$ and a decreasing one for $\gamma < \gamma_{\text{sc}}$. This leads to a general conclusion, that for every α , if there is a bulk transition at $\gamma = \rho_s(\rho_o(\alpha))$, there is a "boundary" transition at $\gamma = \rho_o(\alpha)$. This defines a surface transition line $\gamma = \gamma_{\text{surf}}(\alpha)$ in the low-density phase. The transition is strictly at the boundary because as one crosses the phase boundary, the bulk density profile remains same but the boundary profile changes drastically. Such surface transition is expected to be true generally for all K and also for interacting system, wherever a transition to a shock phase takes place.

In terms of w specified above, the inner solution, in general, has a form

$$\rho_{\text{in}}(\tilde{x}) = \rho_o S_{\text{in}}(\tilde{x}/2w + \xi), \quad (21)$$

with $S_{\text{in}} \rightarrow 1$ as $\tilde{x} \rightarrow -\infty$. The constant, ξ , can be determined from the constraint $S_{\text{in}}(\tilde{x} = 0) = \gamma$ and the explicit form of $F(\rho)$ specified in equation (18). Near the surface transition line ξ has a logarithmic divergence

$$\xi \sim \ln |\gamma - \rho_o|, \quad (22)$$

which leads us to define an exponent ζ_s as

$$\xi \sim |\Delta\alpha|^{\zeta_s}, \quad \text{for } \alpha = \alpha_{\text{surf}} \pm \Delta\alpha. \quad (23)$$

In our case,

$$\zeta_s = O(\log). \quad (24)$$

In the following subsection, we illustrate this general approach for special cases of $K = 1$ and $K \neq 1$.

1. Results for $K = 1$ and $K \neq 1$

Following the above arguments, surface transition lines can be obtained for all values of K . For all K , the explicit inner solution with positive slope at $x = 1$ is

$$\rho_{\text{in}}(\tilde{x}) = \frac{1}{2} + \frac{(1 - 2\rho_o)}{2} \tanh\left[\frac{\tilde{x}}{2w} + \xi\right], \quad (25)$$

where ξ is a constant and

$$w = 1/(1 - 2\rho_o). \quad (26)$$

This solution appears for $\gamma > \rho_o$.

As $\tilde{x} \rightarrow \infty$, the inner solution saturates to $\rho_s = 1 - \rho_o$. The bulk transition to the shock phase occurs when the saturation value, ρ_s , of the surface layer, is smaller than γ . The phase boundary between the low-density and the shock-phase is, therefore, given by the equation $1 - \rho_o(\alpha) = \gamma$. The surface transition to a boundary layer of negative slope occurs when $\gamma < \gamma_{\text{sc}} = \rho_o$. The boundary layer, in this case is

$$\rho = \frac{1}{2} + \frac{1 - 2\rho_o}{2} \coth\left[\left(\frac{\tilde{x}}{2w} + \xi\right)\right], \quad (27)$$

where w is same as in equation (26). w and ξ together determine the position of the "virtual origin" at which the argument of the inner solution vanishes. This is simply in the sense of mathematical continuation since the virtual origin may lie well beyond the physical range of x , $\{0, 1\}$, with an unphysical value of the density.

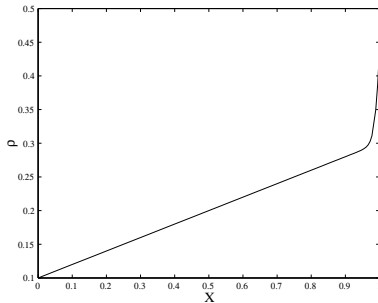


FIG. 3: Density profile with positive slope at the right boundary for $K = 1$ with $\alpha = .1$, $\gamma = .44$, $\epsilon = .0035$ and $\Omega = .2$.

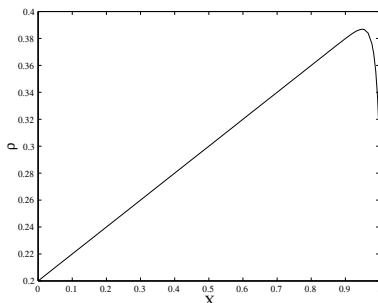


FIG. 4: Density profile with negative slope at the right boundary for $K = 1$ with $\alpha = .2$, $\gamma = .3$, $\epsilon = .0035$ and $\Omega = .2$.

For $K = 1$, using $\rho_o = \Omega + \alpha$, we find

$$w = 1/(1 - 2\Omega - 2\alpha). \quad (28)$$

Further, the constraint $\rho_{in}(\tilde{x} = 0) = \gamma$, leads to

$$\xi = \frac{1}{2} \log \left[\frac{\gamma - \Omega - \alpha}{1 - \Omega - \alpha - \gamma} \right]. \quad (29)$$

for tanh type surface layer (see figure 3) and

$$\xi = \frac{1}{2} \log \left[\frac{\gamma - (\Omega + \alpha)}{\gamma - (1 - \Omega - \alpha)} \right] \quad (30)$$

for coth boundary layer (see figure 4). The surface transition from the tanh type surface layer to the coth type boundary layer takes place if $\gamma < \gamma_{sc} = \rho_o = \Omega + \alpha$ leading to a linear surface transition line, $\gamma = \Omega + \alpha$, on the $\alpha - \gamma$ plane. As this line is approached from either of the two low-density phases, ξ diverges logarithmically as

$$\xi \sim \log |\gamma - \Omega - \alpha|. \quad (31)$$

The surface transition line $\rho_o(\alpha) = \gamma$ and the shock phase boundary $\rho_s = 1 - \rho_o(\alpha) = \gamma$ intersect at $\rho_o = 1/2$.

This intersection point is, therefore, also the critical point (α_c, γ_c) at which $w(\alpha)$ diverges. For $K = 1$, the critical point is $(1/2 - \Omega, 1/2)$. For $\gamma < \gamma_c$, this boundary layer with negative slope at $x = 1$ cannot shocken if α is increased. However, as α is increased, this decaying boundary layer continues to be there in the low-density maximal-current (LM) phase.

For $K \neq 1$, ρ_o is the solution of $g(\rho_o) = \Omega + g(\alpha)$ with $g(\rho)$ given in equation (14). In this case, therefore, the surface transition line $\gamma = \gamma_{sc} = \rho_o$ is determined from the solution for γ from the equation

$$g(\gamma) = \Omega + g(\alpha). \quad (32)$$

The condition for shock formation from a low-density phase with tanh type boundary layer, on the other hand, leads to a phase boundary given by the solution of the equation

$$g(1 - \gamma) = \Omega + g(\alpha). \quad (33)$$

The solutions for γ from equations (32) and (33) are

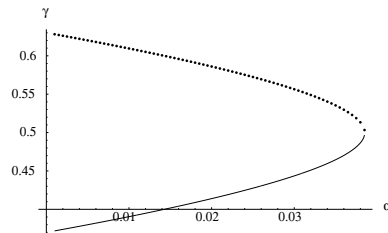


FIG. 5: Solid line represents the surface transition line in the low-density phase for $K = 3$ and $\Omega = .1$. The dotted line corresponds to the phase boundary between the low-density and the shock phase. The intersection of the two lines is the critical point (α_c, γ_c) .

symmetric around $\gamma = 1/2$ (see figure 5) and the intersection of the two solutions at $\gamma = \gamma_c = 1/2$ is the critical point (α_c, γ_c) where

$$g(\gamma_c) = \Omega + g(\alpha_c). \quad (34)$$

Since the surface transition line is symmetric to the phase boundary between the shock and the low-density phases, shapes of these two lines close the critical point are same [10]. The shape of the surface transition line can be obtained independently by substituting $\gamma = \gamma_c - \Delta\gamma$ and $\alpha = \alpha_c - \Delta\alpha$ in equation (32) and expanding it in small $\Delta\gamma$ and $\Delta\alpha$. This leads to a general equation

$$g'(\gamma_c)\Delta\gamma - g''(\gamma_c)(\Delta\gamma)^2/2 + \dots = g'(\alpha_c)\Delta\alpha. \quad (35)$$

Since for $K \neq 1$, $g'(\gamma_c) = 0$, the shape of the surface transition line near the critical point is given by $\Delta\gamma \sim \Delta\alpha^{\chi_-^s}$ with

$$\chi_-^s = 1/2. \quad (36)$$

Similar to the $K = 1$ case, the coth boundary layer, in the low-density phase, leads way to a decaying boundary layer in the shock phase for $\gamma < \gamma_c$.

The mechanism for the formation of the shock for $\gamma > \gamma_c$, is different from that for $\gamma < \gamma_c$, since in the latter case, there is no tanh type boundary layer to be deconfined to form a shock. The effective boundary condition for shock formation, for $\gamma < \gamma_c$ is same as $\gamma = \gamma_c$ since the right branch of the outer solution satisfies this effective boundary condition at its right edge. The original boundary condition $\rho(x = 1) = \gamma$ with $\gamma < \gamma_c$ is satisfied finally with a decaying boundary layer. As a consequence of this, α_c continues to be the critical value of α for shock formation for all $\gamma < \gamma_c$ leading to a vertical phase boundary between the low-density and the shock phase. As α increases in the shock phase, the discontinuity, formed at $x = 1$, moves towards $x = 0$ till it reaches the other end at the high-density-shock phase boundary. Whereas for $\gamma > \gamma_c$, the deconfined boundary layer or the shock at $x = 1$ has a finite height, for $\gamma < \gamma_c$, the shock height increases continuously from zero to a finite value as α is increased. Although the mechanism of shock formation is different for $\gamma > \gamma_c$ and $\gamma < \gamma_c$, the discontinuity is always described by a tanh type inner solution. Alternatively, for all values of γ , the emergence of shock, as one approaches the shock phase from the high-density side, is through the deconfinement of a tanh boundary layer of finite height at $x = 0$. As a consequence of this, the high-density-shock phase-boundary cannot have any critical point on it.

The entire process of surface transition and then shock formation by changing γ for a given α can be understood on a more physical ground. In the low-density phase, for small γ , the withdrawal rate at $x = 1$ is high. Since the bulk dynamics is completely controlled by hopping and adsorption/desorption kinetics, a large withdrawal rate with a fixed α , causes particle depletion at $x = 1$ to be described by a "virtual origin" somewhere at $x > 1$. As γ is increased, the withdrawal rate decreases and we reach a situation where there is neither any depletion nor any accumulation of particles at the end. The "virtual origin" is shifted to ∞ now. If γ is increased further, the withdrawal rate is too slow to get rid of particles that bulk dynamics can feed. This leads to an accumulated region at the boundary until a stage where this accumulated region becomes macroscopic. Beyond this point, the withdrawal rate controls the density near the end and the injection rate controls the remaining part of the density with the two parts joined through a shock or discontinuity.

B. High-density phase

1. $K = 1$

For $K = 1$, the H-phase can be completely understood from the knowledge in L-phase by exploiting the particle-hole symmetry. In this sense, the high-density phase for particles is equivalent to the low-density phase for holes with density profile same as that in figure 3 or figure 4

when the coordinates are transformed as $x \rightarrow 1 - x$. In this transformed coordinates, above the line $\gamma = \Omega + \alpha$, we have the density profile for holes same as figure 3. The boundary layer here is described by equation (25) with the constants

$$w = 1/(2\gamma - 2\Omega - 1) \quad \text{and} \quad (37)$$

$$\xi = \frac{1}{2} \log[(\gamma - \Omega - \alpha)/(\gamma + \alpha - 1 - \Omega)]. \quad (38)$$

It is straightforward to verify that in original coordi-

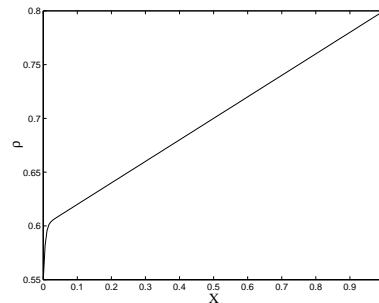


FIG. 6: Density profile with positive slope at the left boundary for $K = 1$ with $\alpha = .55$, $\gamma = .8$, $\epsilon = .001$ and $\Omega = .2$.

nates, the particle density profile appears as figure 6. It consists of a linear profile satisfying the right boundary condition and a boundary layer as in equation (25) with

$$\xi = \frac{1}{2} \log[(\gamma + \alpha - 1 - \Omega)/(\gamma - \Omega - \alpha)], \quad (39)$$

and w same as in (37). The particle-hole symmetry also guarantees a surface phase transition in the high-density phase across $\gamma = \Omega + \alpha$ line. The tanh type boundary

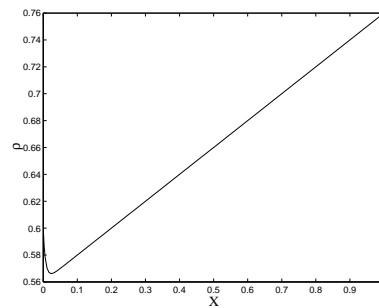


FIG. 7: Density profile with negative slope at the left boundary for $K = 1$ with $\alpha = .6$, $\gamma = .76$, $\epsilon = .001$ and $\Omega = .2$.

layer at $x = 0$ with positive slope changes to a boundary layer with negative slope (see figure 7) described by equation (27) with constants that can be determined using the symmetry.

2. $K \neq 1$

The high-density phase can be divided into two major parts. For $\gamma < \gamma_c = 1/2$, the density profile has bound-

ary layers on both the ends. In addition to a tanh type boundary layer at $x = 0$, there is a decaying boundary layer at $x = 1$. The right boundary layer helps the density profile satisfy the boundary condition at $x = 1$ from a value $\rho = 1/2$. Thus as in the case of shock phase with $\gamma < 1/2$, the effective boundary condition on the right edge for the outer solution continues to be $\rho = 1/2$ in this part of the H phase. In the other part of the H phase, the density profile has only one tanh boundary layer at $x = 0$.

The transition to the shock phase from the high-density phase takes place through the deconfinement of the inner solution

$$\rho = 1/2 + \frac{(2\rho'_o - 1)}{2} \tanh\left[\frac{(2\rho'_o - 1)\tilde{x}}{2} + \xi\right], \quad (40)$$

at $x = 0$. Here $\rho'_o = \rho_{2,\text{out}}(x = 0)$ is the value of the outer solution at $x = 0$. For $\gamma > 1/2$, the outer solution obeying the boundary condition $\rho(x = 1) = \gamma$ can be obtained by solving

$$g(\rho'_o) = -\Omega + g(\gamma). \quad (41)$$

For $\gamma < 1/2$, the outer solution satisfies the effective boundary condition $\rho(x = 1) = 1/2$ and it is the solution of the equation

$$g(\rho'_o) = -\Omega + g(1/2). \quad (42)$$

The boundary layer deconfines, whenever α is smaller than $1 - \rho'_o$, the saturation value of the inner solution in equation (40). This leads to the high-density-shock phase boundaries,

$$g(1 - \alpha) = -\Omega + g(1/2) \quad \text{for } \gamma < 1/2 \quad (43)$$

$$g(1 - \alpha) = -\Omega + g(\gamma) \quad \text{for } \gamma > 1/2. \quad (44)$$

Since for $\gamma < 1/2$, the value of the critical α does not depend on γ , the phase boundary is vertical for all $\gamma < 1/2$, with a K dependent value of α .

Across the surface transition line, the slope of the boundary layer at $x = 0$ changes sign. If the value of ρ'_o is larger than α , a boundary layer with a positive slope at $x = 0$ is expected. In the reverse situation, one expects a boundary layer with a negative slope at $x = 0$. The transition lines are, therefore, given by

$$g(\alpha) = -\Omega + g(1/2) \quad \text{for } \gamma < 1/2, \quad (45)$$

$$g(\alpha) = -\Omega + g(\gamma) \quad \text{for } \gamma > 1/2. \quad (46)$$

The surface transition lines in equations (45) and (46) are represented by dashed lines 1 and 2, respectively, in figure 2. These two lines meet at $\gamma = 1/2$ with a value of α that depends on K . The surface transitions across both the lines are associated with the divergence of ξ and there is no critical point on these lines.

C. Boundary layers in LM and HM phases for $K = 1$

For $K = 1$, $\alpha = 1/2 - \Omega$ and $\gamma = 1/2 + \Omega$ are the boundaries for the low-density and high-density phases respectively since tanh or coth type boundary layers are no more valid on these lines. The LM phase and the symmetrically opposite HM phase appear in the regimes $\{1/2 - \Omega < \alpha < 1/2, \gamma < 1/2\}$ and $\{\alpha > 1/2, 1/2 < \gamma < 1/2 + \Omega\}$ respectively. In the LM phase (see figure

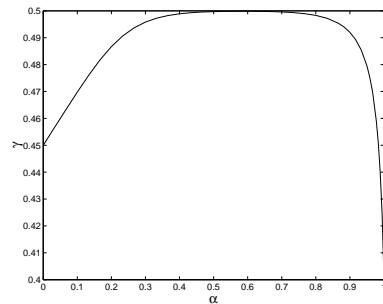


FIG. 8: Density profile in the low-density maximal current (LM) phase with $\alpha = .45$, $\gamma = .4$, $\epsilon = .002$ and $\Omega = .2$.

8), the linear profile, $\rho(x) = \Omega x + \alpha$, satisfies the left boundary condition and continues till $x_{cl} = (1/2 - \alpha)/\Omega$ where $\rho(x_{cl}) = 1/2$. The constant profile continues till the other end where a boundary layer finally satisfies the boundary condition. In the HM phase (see figure 9), the

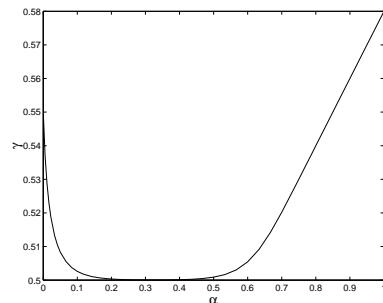


FIG. 9: Density profile in the high-density maximal current (HM) phase with $\alpha = .55$, $\gamma = .58$, $\epsilon = .001$ and $\Omega = .2$.

linear profile satisfying the right boundary condition ends at $x_{ch} = (1 - 2\gamma + 2\Omega)/2\Omega$ with constant density profile for $x < x_{ch}$ and a boundary layer at $x = 0$. To obtain the boundary layer near $x = 1$ (or $x = 0$) for LM (or HM) phase, it is useful to express equation (3) in terms of

$$f(x^*) = (2\rho - 1)/\sqrt{\epsilon}, \quad (47)$$

with $x^* = (x - x_0)/\sqrt{\epsilon}$, where x_0 , as before, represents the center of the solution. In terms of $f(x^*)$, the new equation is

$$\frac{1}{2} \frac{\partial^2 f}{\partial x^{*2}} + \frac{f}{2} \frac{\partial f}{\partial x^*} - \Omega f = 0. \quad (48)$$

A phase plane analysis of equation (48) is useful to identify the appropriate inner solution that can satisfy the boundary conditions. Since the details of such analysis can be found in [11] or in other mathematics textbooks, we briefly mention the basic principles and obtain the contour-plot (figure 10) in an Appendix. Denoting $\frac{df}{dx^*} = p$, we have

$$\frac{dp}{df} = f \frac{2\Omega - p}{p}. \quad (49)$$

To obtain the boundary layer at $x = 1$ for the LM phase, we require the specific solution which satisfies the boundary conditions $\rho(x^*) = 1/2$, as $x^* \rightarrow -\infty$ and $\rho(x^*) = \gamma$ as $x \rightarrow 1$. These conditions are fulfilled by the contour marked with an arrow in figure 10. The origin ($f = p = 0$) is a fixed point for the differential equations and a simple linearization around this fixed point leads to $p = (2\Omega)^{1/2}f$. The approach to $\rho = 1/2$ as $x^* \rightarrow -\infty$ is, therefore, exponential as

$$f \sim \exp[(2\Omega)^{1/2}x^*]. \quad (50)$$

Away from the fixed point ($f = p = 0$), the solution of the differential equation is $f^2 \sim -2p$, implying $f \sim 2/x^*$, as $x^* \rightarrow 0$. The boundary condition $\rho(x = 1) = \gamma$ further leads to $x_0 = 1 - \frac{2\epsilon}{2\gamma - 1}$. As $x \rightarrow 1$, the density profile thus has an algebraic decay as

$$\rho(x) = \frac{1}{2} + \frac{\epsilon}{x - 1 + 2\epsilon/(2\gamma - 1)}. \quad (51)$$

For the HM phase, the boundary layer at the left edge has to be described by the specific solution that satisfies the boundary condition at $x = 0$ and approaches 0 exponentially as $x^* \rightarrow \infty$. It can be shown that this solution is the same as (51) near $x = 0$, with $x_0 = \frac{2\epsilon}{1 - 2\alpha}$. The matching between the linear and the constant profile around x_{cl} or x_{ch} can also be done by choosing the appropriate solution from the contour plot. In the case of LM phase, this solution should merge to the linear one for $x^* \rightarrow -\infty$ and, approach 0 exponentially as $x^* \rightarrow \infty$, with the same length scale as in equation (50). Similar analysis is suitable also for the maximal current(M) phase, that appears for $\alpha > 1/2$ and $\gamma < 1/2$. In this phase, the density profile is fixed at $1/2$ over the entire lattice except for decaying boundary layers same as those in LM and HM phases at $x = 1$ and $x = 0$, respectively.

IV. APPROACH TO VARIOUS PHASE BOUNDARIES

Our final aim is to study the boundary layers for $K = 1$ as different phase boundaries are approached. As the phase boundary $\alpha = 1/2 - \Omega$ is approached from the low-density side (along path 2), $w\xi$ approaches a finite value $1/(2\gamma - 1)$ which diverges as the special point $\gamma = 1/2$ is approached. Since at this special point, $\Omega + \alpha =$

$\gamma = 1/2$, the linear profile satisfies both the boundary conditions and there is no need of any boundary layer. Since $\coth x \sim 1/x$ as $x \rightarrow 0$, there is an algebraically decaying inner solution

$$\rho(x) = \frac{1}{2} + \frac{\epsilon}{x - 1 + 2\epsilon/(2\gamma - 1)}, \quad (52)$$

near the phase boundary $\alpha = 1/2 - \Omega$ for $\gamma < \gamma_c$ as $x \rightarrow 1 - \frac{2\epsilon}{2\gamma - 1}$. This decay is exactly the same as that we find in the density profile in equation (51) that describes the boundary layer in the LM phase (on the other side of the phase boundary, $\alpha = 1/2 - \Omega$). From this analysis, it becomes clear, how the coth boundary layer transforms to an algebraically decaying boundary layer appropriate for LM phase across the phase boundary. As $\tilde{x} \rightarrow -\infty$, the coth inner solution in the L-phase approaches $\rho_o = \Omega + \alpha$ exponentially as

$$\rho(\tilde{x}) = \Omega + \alpha - (1 - 2\Omega - 2\alpha)e^{2[(1 - 2\Omega - 2\alpha)\tilde{x}/2 + \xi]}, \quad (53)$$

with a length scale $1/(1 - 2\Omega - 2\alpha)$ that diverges as the phase boundary $\alpha = 1/2 - \Omega$ is approached. It is interesting to note that as the phase boundary is approached, the algebraic decay of the inner solution near $x = 1$ is same in both L and LM phases. The approach of the two inner solutions in L and LM phases to the bulk density, on the other hand, is exponential with two different length scales. Further, x_0 diverges as $x_0 \sim (2\gamma - 1)^{-1}$ as one approaches the LM and LMH phase boundary along path (3). Situation is symmetric as one approaches the HM and H phase boundary. As the phase boundary $\alpha > 1/2$ and $\gamma = 1/2 + \Omega$ is approached from the H phase along path (4), ξw in the coth boundary layer at $x = 0$ approaches $1/(2\alpha - 1)$. The power-law decay of the boundary layer near $x = 0$ as

$$\rho(x) = \frac{1}{2} + \frac{\epsilon}{x - 2\epsilon/(1 - 2\alpha)} \quad (54)$$

is the same as that for the boundary layer in HM phase. As HM or LM phases are approached from M phase, the boundary layer at $x = 1$ or at $x = 0$, respectively, disappears and a linear profile at the respective edge starts appearing. This is marked by the divergences of x_0 as $(2\gamma - 1)^{-1}$ or $(2\alpha - 1)^{-1}$ along path (5) or (6) respectively.

V. SUMMARY

In summary, we have shown that various bulk phase transitions in particle nonconserving asymmetric simple exclusion processes with open boundaries are associated with divergences of various length scales related to the boundary layers of the density profile. The nature of the divergences are obtained by implementing the techniques of boundary layer analysis on the mean-field equation for the steady-state density profile. In addition to this, we

also show that the low- and high-density phases exist in two different surface phases with distinctly different surface layers in the density profile.

APPENDIX A: PHASE-PLANE ANALYSIS FOR EQUATION (48)

In terms of p and f , second order equation (48) can be decomposed into two coupled first order equations

$$\frac{df}{dx^*} = p \quad \text{and} \quad (\text{A1})$$

$$\frac{dp}{dx^*} = f(2\Omega - p). \quad (\text{A2})$$

$(f = p = 0)$ is a fixed point for these equations. Linearization around this fixed point leads to the following matrix equation

$$\frac{d}{dx^*} \begin{pmatrix} \delta f \\ \delta p \end{pmatrix} = \begin{pmatrix} 0 & 1 \\ 2\Omega & 0 \end{pmatrix} \begin{pmatrix} \delta f \\ \delta p \end{pmatrix}, \quad (\text{A3})$$

which can be solved through standard diagonalization scheme. The eigen vectors corresponding to the

eigenvalues $(2\Omega)^{1/2}$ and $-(2\Omega)^{1/2}$ are $\begin{pmatrix} 1 \\ (2\Omega)^{1/2} \end{pmatrix}$ and $\begin{pmatrix} 1 \\ -(2\Omega)^{1/2} \end{pmatrix}$ respectively. In the following, we present the contour-plots in $f - p$ plane for different boundary conditions.

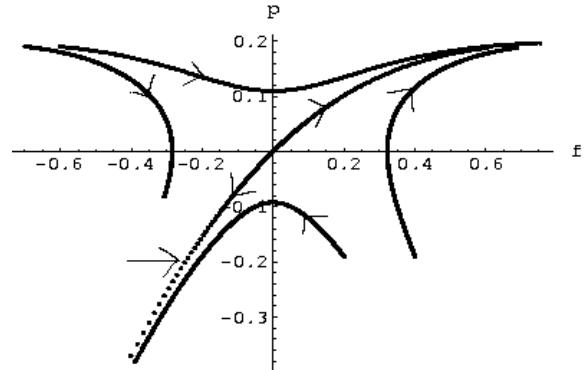


FIG. 10: Contour plots from equations (A1) and (A2) with $\Omega = .1$. The arrows on different contours indicate directions of increasing x^* .

-
- [1] G. M. Schuetz, in *Phase Transitions and Critical Phenomena*, edited by C. Domb and J. Lebowitz (Academic, London, 2000), Vol. 19.
 - [2] T. Ligett, *Interacting Particle Systems: Contact, Voter and Exclusion Processes* (Springer-Verlag, Berlin, 1999)
 - [3] M. R. Evans *et. al.*, Phys. Rev. Lett. **74**, 208 (1995).
 - [4] B. Derrida *et. al.*, J. Phys. A **26**, 1493 (1993); G. Schütz and E. Domany, J. Stat. Phys. **72**, 277 (1993).
 - [5] G. Tripathy and M. Barma, Phys. Rev. Lett. **78**, 3039 (1997); Phys. Rev. E **58**, 1911 (1998).
 - [6] M. R. Evans *et. al.*, Phys. Rev. Lett. **74**, 208 (1995); J. Stat. Phys. **80**, 69 (1995).
 - [7] J. Krug, Phys. Rev. Lett. **67**, 1882 (1991); J. S. Hager *et. al.*, Phys. Rev. E **63** 056110 (2001).
 - [8] A. Parmeggiani, T. Franosch and E. Frey, Phys. Rev. Lett. **90**, 086601 (2003); cond-mat/0408034; M. R. Evans, R. Juhasz and L. Santen, Phys. Rev. E **68**, 026117 (2003).
 - [9] S. Klumpp and R. Lipowsky, Eur. Phys. Lett. **66**, 90 (2004); J. Stat. Phys. **113**, 233 (2003).
 - [10] Sutapa Mukherji and Somendra M. Bhattacharjee, J. Phys. A **38**, L285 (2005).
 - [11] Julian D. Cole, *Perturbation Methods in Applied Mathematics* (Blaisdell Publishing, Massachusetts, 1968).